

# Resonant tunneling and intrinsic bistability in asymmetric double-barrier heterostructures

A. Zaslavsky, V. J. Goldman,<sup>a)</sup> and D. C. Tsui

Department of Electrical Engineering, Princeton University, Princeton, New Jersey 08544

J. E. Cunningham

AT&T Bell Laboratories, Holmdel, New Jersey 07788

(Received 13 June 1988; accepted for publication 1 August 1988)

We report measurements of the current-voltage characteristics of an asymmetric GaAs/AlGaAs double-barrier resonant tunneling device. The structure was designed to increase the space charge in the well under forward bias and consequently enhance the electrostatic feedback that leads to intrinsic bistability. The magnetotunneling data demonstrate unambiguously that the observed bistability is the property of the device, rather than the biasing circuit.

Now that some of the more basic aspects of charge transport in double-barrier resonant tunneling structures (DBRTS's) have been addressed both theoretically<sup>1-4</sup> and experimentally,<sup>5-8</sup> other, more subtle phenomena associated with such tunneling have attracted attention. One such phenomenon is the intrinsic bistability in DBRTS caused by the space-charge formation in the well.<sup>9</sup> The space charge alters the bias distribution over the structure which, in turn, alters the tunneling current density and may produce two different states of the system in some range of bias voltage. Experimental evidence for intrinsic bistability in DBRTS's has been reported previously,<sup>9</sup> but this report has also been challenged.<sup>10</sup> Here we present a further study of intrinsic bistability in an asymmetric GaAs/Al<sub>x</sub>Ga<sub>1-x</sub>As DBRTS. The data, obtained from low-temperature current-voltage ( $I$ - $V$ ) and differential conductance ( $dI/dV$ ) measurements in a magnetic field, indicate unambiguously that two current states exist in the bistable regime.

Since intrinsic bistability is produced by electrostatic feedback of the space charge dynamically stored in the well of a DBRTS, it is helpful to increase the well charge density  $\sigma_w$ . A practical method of achieving this is to enlarge the collector barrier. To this end an asymmetric DBRTS was designed with one of the barriers significantly higher than the other.<sup>11</sup> In our device under forward bias the higher collector barrier increases the time electrons spent in the well, while the lower emitter barrier keeps the current density reasonably large (the current density is mostly determined by the transmission coefficient of the emitter barrier<sup>3,9</sup>). Under reverse bias the barrier asymmetry has the opposite effect: peak current density is low and little space charge is built up in the well.

Our structure was grown by molecular beam epitaxy on an  $n^+$   $\langle 100 \rangle$  GaAs substrate at a relatively low temperature of 620 °C in order to limit dopant (Si) diffusion. We estimate the active region of our device to consist of (i) 0.4  $\mu\text{m}$  of GaAs Si doped to  $\sim 2 \times 10^{17} \text{ cm}^{-3}$ , (ii) 120 Å of undoped GaAs, (iii) 90 Å of Al<sub>0.42</sub>Ga<sub>0.58</sub>As (lower barrier), (iv) 56 Å GaAs (well), (v) 90 Å of Al<sub>0.58</sub>Ga<sub>0.42</sub>As (higher barrier), (vi) 60 Å of undoped GaAs, (vii) finally, 0.4  $\mu\text{m}$  of  $n$

$\sim 2 \times 10^{17} \text{ cm}^{-3}$  GaAs. The barriers and the well were undoped and the spacer layers were grown on both sides of the barriers to reduce Si diffusion into the undoped region. The devices were defined by  $2 \times 10^{-5} \text{ cm}^2$  AuNiGe circular dots and mesa etched. Good ohmic contacts resulted from 45 s of alloying in hydrogen at 400 °C.

All measurements reported here were done at about 1 K by the pseudo-four-terminal technique with a 1.5 nF capacitor in parallel with and close to the device. The  $I$ - $V$  characteristic of the asymmetric DBRTS is shown in Fig. 1(a). The reverse bias characteristic exhibits a high, 20:1 peak to valley ratio, with the current threshold occurring at  $V_{\text{th}} \approx -200$  mV and the peak occurring at  $V_p = -265$  mV. In the forward bias characteristic,  $V_{\text{th}}$  also falls near 200 mV but the peak voltage  $V_p$  is shifted to 565 mV. Between 510 mV and  $V_p$  the DBRTS is in a bistable regime: depending on the voltage sweep direction the device is either in a high- or a low-current state. The ratio of the peak current under forward bias to that under reverse bias is about 16:1. Both forward and reverse  $I$ - $V$  characteristics exhibit phonon-assisted tunneling features after the resonant tunneling peaks.<sup>12</sup> At 620 mV forward bias the current begins to increase sharply, whereas under reverse bias the current valley persists until 0.9 V (further application of reverse bias results in a second, less pronounced current peak at 1.15 V, not shown).

The band diagram of our device under forward and reverse bias is shown in Figs. 1(b) and 1(c). The Fermi energy in the electrodes  $E_F$  is  $\sim 20$  meV. The energy  $E_0$  of the resonant subband, measured from the bottom of the well, is 80 meV (taking into account band nonparabolicity). The quantity  $\Delta E$  is defined as the energy separation between  $E_0$  and the emitter  $E_F$  (in our sign convention  $\Delta E$  is negative at zero bias). As bias is applied to the device,  $\Delta E$  becomes less negative. In the sequential tunneling picture,<sup>3</sup> electrons begin to tunnel resonantly into the well when the applied bias lines up  $E_0$  and the emitter  $E_F$  (that is, when  $\Delta E = 0$ ), allowing tunneling that conserves both energy and transverse momentum. As more bias is applied, tunneling current continues to increase until subband  $E_0$  lines up with the bottom of the conduction band in the emitter ( $\Delta E = E_F$ ), at which point energy and momentum conserving tunneling becomes impossible and the device switches to the low current state.

<sup>a)</sup> Present and permanent address: Department of Physics, SUNY at Stony Brook, Stony Brook, NY 11794.

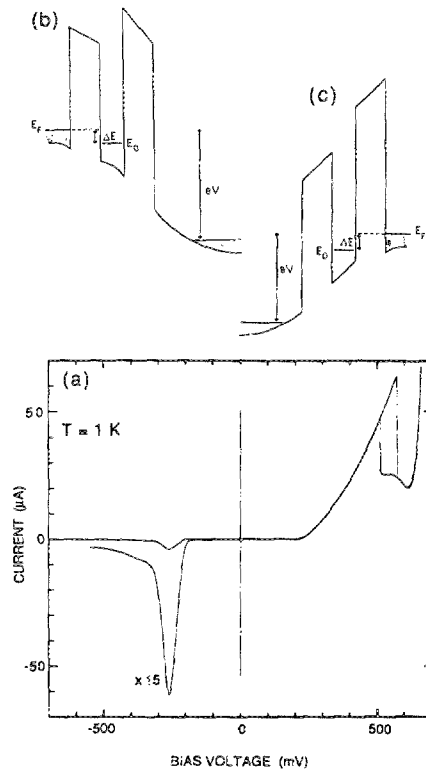


FIG. 1. (a)  $I$ - $V$  characteristic of the asymmetric DBRTS device described in the text. Also shown is an expansion of the negative bias range. (b), (c) Schematic conduction-band diagrams of the device under forward (b) and reverse (c) bias.

In the resonant tunneling regime a space charge  $\sigma_w$  is present in the well<sup>8</sup>:

$$\sigma_w \approx \hbar J / T_c E_0,$$

where  $J$  is the current density and  $T_c$  is the transmission coefficient of the collector barrier. The space charge in the well increases the electric field in the collector barrier and reduces the lowering of the resonant subband with respect to the emitter. Under forward bias, the higher collector barrier (that is, smaller  $T_c$ ) of our device enhances charge storage in the well. In the bistable region space charge  $\sigma_w$  is very large, reaching  $4.5 \times 10^{11}$  electrons/cm<sup>2</sup> at  $V_p$ , nearly a factor of 5 more than in the symmetric DBRTS discussed in Ref. 8. This explains the shift of the forward bias  $V_p$  out to 565 mV: once the tunneling current and hence the space charge  $\sigma_w$  become appreciable, only a fraction of the incremental applied bias contributes to increasing  $\Delta E$ . Under reverse bias the tunneling current is small and the collector barrier is low; space charge  $\sigma_w$  is accordingly negligible and does not effectively screen the external electric field. Hence the much lower value of reverse bias  $V_p = 265$  mV is compared to the forward bias.

In order to gain a better understanding of our system and to study the bistable region, we measured the differential conductance  $dI/dV$  of our DBRTS in magnetic fields  $B$  up to 10.5 T ( $B$  parallel to the direction of tunneling). The measurements were carried out by the standard ac modulation technique with lock-in detection. Both fixed voltage (swept magnetic field) and fixed  $B$  (swept voltage) measurements were done. Three typical forward bias  $dI/dV$  vs  $V$  traces at

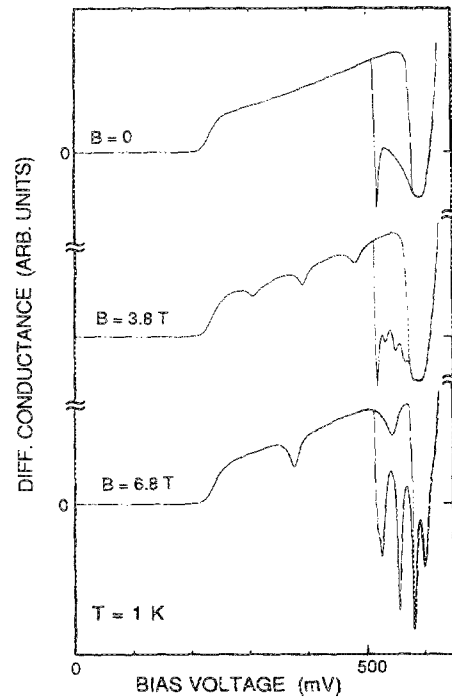


FIG. 2. Representative traces of  $dI/dV$  vs  $V$  at constant  $B$ .

constant  $B$  are shown in Fig. 2. The magnetic field induces an oscillatory behavior in the  $B = 0$  differential conductance. At higher  $B$  the conductance minima become sharper and deeper. The bias spacing between  $dI/dV$  minima increases with  $B$ . The behavior of magnetoquantum oscillations in the high- and low-current states is unambiguously different. The bias spacing between oscillations in the high-current state is larger by a factor of  $\sim 6$ . This ratio persists at all values of  $B$ . This difference in the bias spacing is due to the screening of the voltage drop in the emitter barrier by  $\sigma_w$ . In the high current state  $\sigma_w$  is much higher and screens the external electric field more effectively.

In Fig. 3 we show the  $dI/dV$  vs  $B$  plots of the high- and low-current states at the same bias ( $V = 540$  mV) in the bistable region. Once again, the oscillatory behavior of  $dI/dV$  in the two states is evidently different. The large number of clearly visible conductance minima indicates the good quality of the device. The regularity and sharpness of  $dI/dV$  features argues against the possibility of biasing circuit oscillations. Moreover, conductance measurements done with two different biasing circuit configurations yielded identical results.

The magnetoquantum oscillations induced in the  $dI/dV$  of DBRTS are due to the Landau quantization of electrons in the well.<sup>6,8</sup> In the high-current state, where tunneling conserves energy, the minima in the conductance occur when the emitter  $E_F$  lines up with the minima in the Landau-quantized density of states. In the low-current state the current is a combination of LO-phonon-emission-assisted tunneling and momentum-nonconserving but elastic tunneling via ionized impurity scattering.<sup>12</sup> In our device the magnetoquantum oscillations in the low-current state occur in the LO-phonon-assisted component.<sup>12,13</sup> A full analysis of the

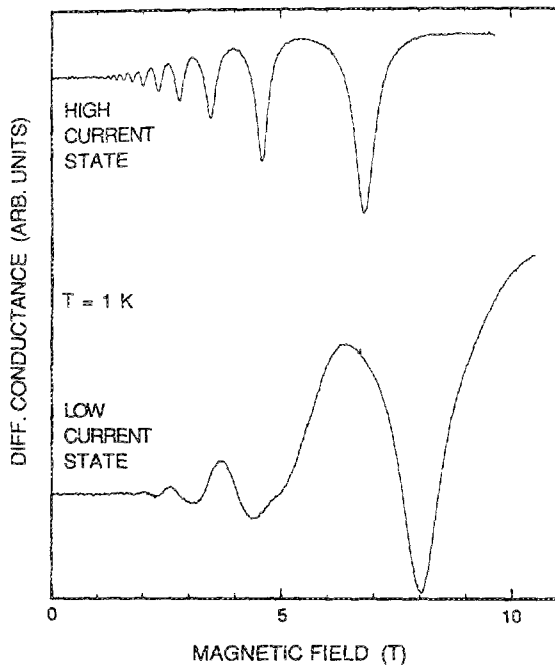


FIG. 3. Traces of  $dI/dV$  vs  $B$  at  $V = 540$  mV in the bistable region.

oscillatory behavior of the high- and low-current states, shown in Figs. 2 and 3, will be reported separately—for now we stress that our data clearly demonstrate the existence of two states in the bistable region.

We note here that the series resistance arising from the ohmic contacts, the doped electrodes, and the substrate is estimated to be a few ohms for our processing procedure. We obtain this value from measurements on similarly processed devices that contained very thin barriers or no barriers at all. The nominally undoped spacer layers near the barriers are, in fact, doped by Si diffusion; in any case, their thickness is about 100 Å which corresponds to half the average separation between Si ions at the  $2 \times 10^{17}$  cm<sup>-3</sup> doping level. Therefore, the voltage drop outside the double-barrier region is insignificant compared to the extent of the bistable region ( $\approx 60$  mV) in this device.

Finally, we would like to address the question of the biasing circuit oscillation in DBRTS. It has been reported that high-frequency oscillation of the biasing circuit can lead to hysteretic and switching behavior superficially similar to intrinsic bistability.<sup>10,14</sup> It is possible, however, to suppress rf oscillation in a high-impedance DBRTS device by means of an external capacitor.<sup>9,15</sup> The maximum oscillation frequency of a DBRTS is limited by its intrinsic  $RC$  time constant: the capacitance and impedance of the emitter barrier determine the charging time of the well. In our device the intrinsic

capacitance is about 20 pF and the minimum resistance [at  $V_p$ , see Fig. 1(a)] is approximately 10 kΩ, so the intrinsic maximum oscillation frequency is  $\sim 5$  MHz. The parallel 1.5 nF external capacitor, installed very close to the device, further reduces this frequency to 60 kHz. At this low frequency the voltage source can maintain a constant applied bias and the rf oscillation does not occur. This is confirmed by the magnetotunneling data in Figs. 2 and 3. Hence the observed bistable  $I$ - $V$  curve of Fig. 1(a) is intrinsic to our device.

In conclusion, we have measured the  $I$ - $V$  characteristics of an asymmetric DBRTS. The enhanced charging of the well in our DBRTS under forward bias made the intrinsic bistability more pronounced and easier to observe, while the high impedance of the device suppressed the possibility of high-frequency biasing circuit oscillation. Our magnetoquantum oscillation data confirm the existence of two current states in the bistable range of bias. Our data also indicate the presence of an LO-phonon-assisted tunneling component in the valley current. The different tunneling mechanisms responsible for the valley current will be the subject of a future study.

The authors gratefully acknowledge computer assistance by Dr. H. P. Wei. The work at Princeton University is supported by the Air Force Office of Scientific Research, the Army Research Office, and a grant from Siemens Research and Technology Laboratory.

<sup>1</sup>R. Tsu and L. Esaki, *Appl. Phys. Lett.* **22**, 562 (1973).

<sup>2</sup>B. Ricco and M. Azbel, *Phys. Rev. B* **29**, 1970 (1984).

<sup>3</sup>S. Luryi, *Appl. Phys. Lett.* **47**, 490 (1985).

<sup>4</sup>T. Weil and B. Vinter, *Appl. Phys. Lett.* **50**, 1281 (1987); W. Frensley, *Phys. Rev. B* **36**, 1570 (1987).

<sup>5</sup>L. L. Chang, L. Esaki, and R. Tsu, *Appl. Phys. Lett.* **24**, 593 (1974).

<sup>6</sup>E. E. Mendez, L. Esaki, and W. I. Wang, *Phys. Rev. B* **33**, 2893 (1986).

<sup>7</sup>M. Reed, J. W. Lee, and H.-L. Tsai, *Appl. Phys. Lett.* **49**, 158 (1986).

<sup>8</sup>V. J. Goldman, D. C. Tsui, and J. E. Cunningham, *Phys. Rev. B* **35**, 9387 (1987).

<sup>9</sup>V. J. Goldman, D. C. Tsui, and J. E. Cunningham, *Phys. Rev. Lett.* **58**, 1256 (1987).

<sup>10</sup>T. C. L. G. Sollner, *Phys. Rev. Lett.* **59**, 1622 (1987).

<sup>11</sup>Data on an asymmetric DBRTS with thin/thick barriers have been reported by V. J. Goldman, D. C. Tsui, and J. E. Cunningham, *Solid-State Electron.* **31**, 731 (1988).

<sup>12</sup>V. J. Goldman, D. C. Tsui, and J. E. Cunningham, *Phys. Rev. B* **36**, 7635 (1987).

<sup>13</sup>L. Eaves, E. S. Alves, T. J. Foster, M. Henini, O. H. Hughes, M. L. Leadbeater, F. W. Sheard, G. A. Toombs, K. Chan, A. Celeste, J. C. Portal, G. Hill, and M. A. Pate (unpublished).

<sup>14</sup>C. A. Payling, E. Alves, L. Eaves, T. J. Foster, M. Henini, O. H. Hughes, P. E. Simmonds, J. C. Portal, G. Hill, and M. A. Pate, *J. Phys. (Paris)* **48**, C5-289 (1987); J. F. Young, B. M. Wood, H. C. Liu, M. Buchanan, D. Landheer, A. J. SpringThorpe, and F. Mandeville, *Appl. Phys. Lett.* **52**, 1398 (1988).

<sup>15</sup>V. J. Goldman, D. C. Tsui, and J. E. Cunningham, *Phys. Rev. Lett.* **59**, 1623 (1987); V. J. Goldman, *Bull. Am. Phys. Soc.* **33**, 254 (1988).